6156 *Macromolecules* **2010**, *43*, 6156–6165
DOI: 10.1021/ma100761a

Macromolecules
ARTICLE

Media-Modulated Interchain or Intrachain Coordination of Amphiphilic Block Copolymer Micelles

Huan Gao, Guhuan Liu, Xuejun Chen, Zhenhua Hao, Jianyu Tong, Lican Lu, and Yuanli Cai*

Key Laboratory of Environmentally Friendly Chemistry and Applications of Ministry of Education, Key Laboratory of Advanced Functional Polymeric Materials of College of Hunan Province, Key Laboratory of Polymeric Materials & Application Technology of Hunan Province, College of Chemistry, Xiangtan University, Xiangtan, Hunan 411105, China

Feng Long and Mingqiang Zhu

State Key Laboratory of Chemo/Biosensing and Chemometrics, Hunan University, Changsha, Hunan 410082, China

Received April 8, 2010; Revised Manuscript Received June 14, 2010

ABSTRACT: Inspired by the tunability of coordination mode of natural zinc proteins, this paper describes a new type of polymer micelle, whose coordination mode may be finely tuned simply via adjusting the solution media. To this end, a well-defined poly[*N*-(6-(3,5-di-*tert*-butyl-2-hydroxybenzylideneamino)hexyl)-methacrylamide]-*block*-poly(2-hydroxyethyl methacrylate) (PDBHHMA-*b*-PHEMA) amphiphilic block copolymer was synthesized via rapid and well-controlled visible light activating RAFT polymerization at 25 °C and subsequently directly reacted with 3,5-di-*tert*-butyl-2-hydroxybenzaldehyde. ^{1}H NMR and GPC analyses indicate the intact structure, well-defined molecular weight, and narrow distribution of $PDBHHMA_{32}$-*b*-$PHEMA_{120}$. $PDBHHMA_{32}$-*b*-$PHEMA_{120}$ may self-assembles into small PDBHHMA-core micelles in methanol or large inversed PDBHHMA-shell micelles in dichloromethane. Cobalt ions coordinate with the functionalities of PDBHHMA blocks in whole micellar shells or cores. The coordination of DBHHMA units in micellar shells proceeds much more rapidly than in micellar cores. The addition of small amount of DMF may significantly accelerate the coordination process in micellar cores. Although this coordination has a negligible effect on the sizes of both types of spherical micelles, coordination in micellar cores leads to a linear increase of light scattering intensity up to a critical feed molar ratio of $[Co^{2+}]_0/[DBHHMA]_0 = 0.4$, whereas coordination in micellar shells does not influence light scattering intensity, even large excess of cobalt ions added, e.g., $[Co^{2+}]_0/[DBHHMA]_0 = 0.7$. In micellar cores, cobalt ions tend to coordinate with DBHHMA units in interchain mode; *N,N*-dimethylformamide (DMF) cosolvent may accelerate this coordination process but increase the tendency of intrachain coordination. On the contrary, coordination in micellar shells occurs predominantly in intrachain mode. These media-tunable coordination modes finely tune the stability of micelles in their nonselective good solvent DMF.

Introduction

The incorporation of noncovalent interactions, e.g. hydrogen bonding,[1−3] ionic complexation,[4,5] or metal−ligand coordination,[6,7] into polymer micelles have opened a pathway toward supramolecular functional polymer nanomaterials. We[8] and other groups[9,10] demonstrated that noncovalent interactions gave rise to some reversible structure and properties of polymer micelles that may be tuned by external stimuli. Among these noncovalent interactions, the metal−ligand coordination is of particular interest because it is highly directional, a wide range of ligands are available, and the interaction strength can be well tuned by choosing appropriate metal ions, ligands, or solvents. More importantly, the metal−ligand coordination facilitates the formation of metal-functionalized polymer micelles, e.g., MoS_x-filled polymer micelles[11] or the continuous and segmented polymer/metal oxide micellar nanowires.[12]

In recent years, Schubert, Gohy, and co-workers did some pioneering work on metal-coordinated polymer micelles.[13−18] They utilized these metallo-supramolecular interactions to modulate the size, conformation, and functionality of coronal chains of polymer micelles,[19,20] convert spherical micelles into the switchable vesicles,[21] prepare spherical or wormlike amphiphilic brush micelles[22] and multicompartment micelles,[23] and fabricate the coordination-crosslinked micellar network.[24]

The polymer micelles may be functionalized as powerful nanocarriers through metal−ligand coordination for a variety of applications. For example, Weberskirch and co-workers[25−27] described the highly active nanoreactors based on the coordinated polymer micelles. Wooley and co-workers[28,29] utilized the coordinated polymer micelles as the imaging and therapeutic agent nanocarriers. Gates and co-workers[30] utilized the coordinated polymer micelles to control the size and shape of gold nanostructures.

Indeed, the metal−ligand coordination is a versatile tool for the formation of functionalized polymer micelles. Stuart and co-workers[31] described the formation of complex-coacervate-core micelles. Recently, O'Reilly and co-workers reported the covalently shell-crosslinked copolymer micelles with metal-coordinated cores[32] and metal-functionalized polymer nanocages with

*Corresponding author: phone +86-731-58298876; Fax +86-731-58292251; e-mail ylcai98@xtu.edu.cn.

 Published on Web 06/29/2010

interior functionality.[33] Harruna and co-workers[34] reported amphiphilic tris(2,2′-bipyridine)ruthenium-cored star-shaped copolymer micelles. Recently, Liang and co-workers[35] reported the formation of Al^{3+}-coordination-stabilized polymer micelles.

Nature uses metal−ligand coordination to construct a variety of elegant supramolecular architectures, which is commonly seen in biological systems. As an archetype of natural supramolecular architectures based on coordination, metalloproteins assemble into well-defined dynamic architectures. These metalloproteins are highly sensitive to their surrounding physiological media in a timely and spatially coordinated manner.[36] For example, according to the surrounding residues of polypeptides and physiological media, zinc ions may bind to the sites within a single polypeptide chain in the intrachain coordination mode or at the interfaces of several polypeptide chains to establish homologous or heterologous protein−protein interactions in the interchain coordination mode.[37] In coordinating sites of zinc enzymes, there are steric constraints in providing space for media substrate, but in the sites of structural zinc protein, there is rarely space for the coordination of an additional ligand.[37] In addition, in zinc sensors, the binding energetics is expected to be linked to conformational changes of the protein for transmission of a signal, while in the sites involved in zinc transport, the ligand environment is expected to generate a site, in which the zinc ion is mobile.[37]

Inspired by this fascinating tunability of coordination mode of natural zinc proteins, this paper explores the tunability of coordination mode in polymer micelles. Accordingly, the tunable coordination in polymer micelles may manipulate stability, permeability, or even catalytic reactivity of functionalized micelles. Clearly, these tunable properties are desirable not only in the chemical related fields such as catalysts or nanoreactors but also for the biomedical-related applications as biosensors or drug carriers. However, to the best of our awareness, the study on tunability of coordination mode in polymer micelles is unprecedented.

This paper describes a new type of polymer micelle, in which the coordination mode may be well tuned simply via adjusting the solution media. To this end, poly[*N*-(6-(3,5-di-*tert*-butyl-2-hydroxybenzylideneamino)hexyl)methacrylamide]-*block*-poly(2-hydroxyethyl methacrylate) (PDBHHMA-*b*-PHEMA) was synthesized for the fabrication of PDBHHMA-core micelles and the inversed PDBHHMA-shell micelles. As shown in Figure 1, because the functionalities of PDBHHMA chains have the semistructural character of the widely studied salen ligands,[38] one portion of cobalt ions may coordinate with two portions of the functionalities of PDBHHMA chains, in either inter- or intrachain mode.

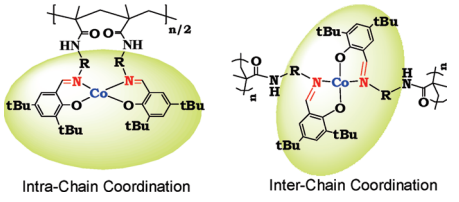

Figure 1. Schemetic illustration of the mode of interchain or intrachain coordination of the functionalities in poly[*N*-(6-(3,5-di-*tert*-butyl-2-hydroxybenzylideneamino)hexyl)methacrylamide] (PDBHHMA) with cobalt ions, where R is hexylene spapcer, *t*Bu is *tert*-butyl group, and Co is the cobalt ion.

The reversible addition−fragmentation chain transfer radical polymerization or RAFT polymerization[39] is a powerful tool for the synthesis of well-defined water-soluble or stimuli-responsive polymers.[40−50] In recent years, our group exploited an environmentally friendly, rapid, and well-controlled visible light activating ambient temperature RAFT polymerization.[51−54] This approach was utilized for the facile synthesis of well-defined water-soluble polymers in alcohol[55,56] or aqueous solution.[57,58] Moreover, this polymerization can immediately start or cease upon light switching on or off and thus may precisely control the molecular weight and distribution of targeted polymers.[58]

As shown in Scheme 1, PDBHHMA-*b*-PHEMA copolymer was synthesized via a sequential visible light activating RAFT polymerization of HEMA monomer and 6-aminohexyl methacrylamide hydrochloride (AHMA) monomer at 25 °C, followed by directly reacting with 3,5-di-*tert*-butyl-2-hydroxybenzaldehyde. This block copolymer was characterized using ^{1}H NMR and gel permeation chromatography (GPC). The coordination kinetics and efficiency of DBHHMA units with cobalt ions in either micellar cores or inversed micellar shells were studied using UV−vis spectroscopy. The effects of coordination on morphology of micelles and the possible coordination mode were investigated using transmission electron microscopy (TEM), dynamic light scattering (DLS), and GPC mesurements.

Experimental Section

Materials. Hexylenediamine was purchased from Yuanji Chemical Co. Hexylenediamine dihydrochloride salt was prepared via adjusting hexylenediamine to pH 1.0 using a 35% hydrochloric acid solution, precipitating from large excess of the mixed solvent of isopropanol and ethyl ether at a volume ratio of 2:1. Methacrylic anhydride (98%, Acros) was used as received. Hydroxyethyl methacrylate (HEMA, Acros, 96%) was distilled under vacuum and stored at −30 °C prior to use. 2-Cyanopropan-2-yl-4-fluorobenzodithioate (CPFDB) was synthesized according to the literature procedures.[59] (2,4,6-Trimethylbenzoyl)-diphenylphosphine oxide (TPO, 97%) was purchased from Runtec Chem. Co. and used as received. Cobalt acetate ($Co(OAc)_2 \cdot 4H_2O$), sodium hydroxide, hydrochloric acid, methanol, dichloromethane (DCM), and *N*,*N*-dimethylformamide (DMF) were purchased from Shanghai Reagent Co. and used as received. Highly pure deionized water at resistivity over 18 MΩ cm^{-1} was utilized. JB400 filters were purchased from Yaguang Sci. Edu. Equip. Co.

Scheme 1. Synthetic Pathway for 6-Aminohexylmethacrylamide Hydrochloride (AHMA) Monomer Salt and the Targeted Poly[*N*-(6-(3,5-di-*tert*-butyl-2-hydroxybenzylideneamino)hexyl)methacrylamide]-*block*-poly(2-hydroxyethyl methacrylate) (PDBHHMA-*b*-PHEMA) Copolymer[a]

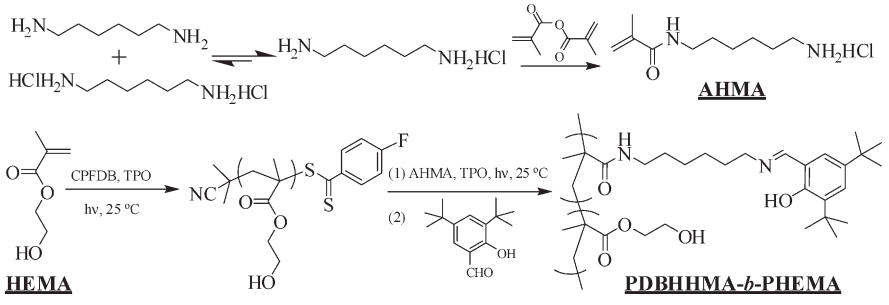

[a] CPFDB is 2-cyanopropan-2-yl-4-fluorobenzodithioate chain transfer agent, and TPO is (2,4,6-trimethylbenzoyl) diphenylphosphine oxide photoinitiator.

Visible Light Source. The light of mercury vapor lamp emitting separately at 254, 302, 313, 365, 405, 436, 545, and 577 nm was filtered by JB400 filters to cut off the shorter wave UV light below 400 nm and adjust the light intensity. Thus, the visible light, emitting separately at 405, 436, 545, and 577 nm, at intensity of 150 μW cm^{-2} at λ = 420 nm, was obtained for the activation of RAFT polymerization at 25 °C.

Synthesis of 6-Aminohexyl Methacrylamide (AHMA) Monomer Hydrochloride Ammonium Salt. Hexylenediamine dihydrochloride salt (14.17 g, 75 mmol), hexylenediamine (18.56 g, 160 mmol), and 200 mL of water were added in a 1000 mL round-bottom flask. After stirring at 25 °C for 1 h, 230 mL of methanol was charged in this flask. The solution was cooled down to −30 °C in an ethanol thermostatic bath. Methacrylic anhydride (23.10 g, 150 mmol) and traces of hydroquinone inhibitor were charged in this flask. The solution was stirred at −30 °C for 1.5 h. Thereafter, the solution was adjusted to pH 1.0 using 35% hydrochloric acid. The solvent was removed by rotary evaporation at 40 °C. The crude creamy product was recrystallized from isopropanol for 3 times to give the final white AHMA amonium salt. Weight: 10.97 g; yield: 33%. ^{1}H NMR (δ, ppm): 5.51 and 5.74 (2H, $\mathbf{CH_2}$=CCH_3), 3.33 (2H, $CONHC\mathbf{H_2}$), 3.07 (2H, $HCl\cdot NH_2C\mathbf{H_2}CH_2$), 2.00 (3H, CH_2=$CHC\mathbf{H_3}$), 1.74 (2H, $CONHCH_2C\mathbf{H_2}$), 1.63 (2H, $HCl\cdot NH_2CH_2C\mathbf{H_2}$), 1.46 (4H, $CONHCH_2CH_2CH_2CH_2CH_2CH_2NH_2\cdot HCl$).

Visible Light Activating RAFT Polymerization of HEMA Monomer at 25 °C. HEMA (19.5 g, 150.0 mmol), CPFDB (179.2 mg, 0.75 mmol), TPO (65 mg, 0.187 mmol), and 15.5 g of DMF were charged in a 100 mL round-bottomed flask. This flask was capped with rubber septa and immersed in a thermostatic water bath at 25 °C. After bubbling with argon gas for 60 min, the solution was irradiated with the visible light for 3.5 h. 52.5% HEMA monomer was polymerized according to ^{1}H NMR analysis. PHEMA was precipitated from large excess of diethyl ether and dried in vacuum overnight. Weight: 7.86 g; yield: 77%. ^{1}H NMR: DP = 120. GPC: M_n = 37.2 kg mol^{-1}, M_w/M_n = 1.09.

Synthesis of PDBHHMA-*b*-PHEMA Copolymer. This copolymer was synthesized via the visible light activating RAFT polymerization of AHMA monomer salt, using the above-synthesized PHEMA as a macromolecular chain transfer agent (macro-CTA) in aqueous solution at 25 °C. The polymerized solution was directly reacted with 3,5-di-*tert*-butyl-2-hydroxybenzaldehyde to give the targeted copolymer.

PHEMA (1.56 g, 0.1 mmol), TPO (6.96 mg, 0.02 mmol), and 4.5 g of DMF were charged in a 50 mL round-bottom flask and stirred until PHEMA was completely dissolved. AHMA (2.205 g, 10 mmol) and 4.5 g of water were added in this flask. The solution was adjusted to pH 1.5−2.0, using 35% hydrochloric acid. This flask was capped with rubber septa and immersed in a thermostatic water bath at 25 °C. After bubbling with argon gas for 60 min, the solution was irradiated with the visible light for 35 min. After this visible light irradiation, 3,5-di-*tert*-butyl-2-hydroxybenzaldehyde (3.10 g, 13.3 mmol) and 30 g of DMF were directly charged in this flask. The solution was adjusted to pH 10, using a 2.5 mol L^{-1} NaOH aqueous solution, stirred at 25 °C for 16 h. The polymer was precipitated from large excess of water. The solids were dissolved in the mixed solvent of 30 g of DMF and 30 g of acetone and further precipitated from large excess of petroleum ether. The solids were dried in vacuum overnight to afford the final PDBHHMA-*b*-PHEMA copolymer. Weight: 2.11 g; yield: 74%. ^{1}H NMR: PDBHHMA$_{32}$-*b*-PHEMA$_{120}$. GPC: M_n = 43.5 kg mol^{-1}, M_w/M_n = 1.13.

Micellization of PDBHHMA$_{32}$-*b*-PHEMA$_{120}$ Copolymer. A typical micellization procedure was as follows: 0.10 g of PDBHHMA$_{32}$-*b*-PHEMA$_{120}$ copolymer was dissolved in 10.0 g of DMF in a flask. 90.0 g of methanol was added dropwise in this flask under stirring at 20 °C. This flask was capped with glass stopper, stirred at 20 °C for 12 h, and kept still for 4 h to afford 1.0 mg g^{-1} methanol solution of PDBHHMA-core micelles. The procedure for the preparation of PDBHHMA-shell micelles in DCM solution was the same except for micellization in DCM.

Coordination of Cobalt Ions in PDBHHMA$_{32}$-*b*-PHEMA$_{120}$ Micellar Solution. Cobalt acetate was dissolved in mixed solvent at the ratio same as micellar solution to $[Co^{2+}]_0 = 1.13 \times 10^{-6}$ mol g^{-1}. This cobalt acetate solution was added dropwise into 1.0 mg g^{-1} micellar solution under stirring. The mixture was stirred in air at 20 °C for 12 h and kept still for 4 h to ensure the fulfillment of coordination.

One portion of solution was diluted to a copolymer concentration of 0.125 mg g^{-1} at the same solvent ratio as initial solution and kept still for 4 h prior to UV−vis spectroscopic measurements; one portion of solution was diluted to 0.5 mg g^{-1} at the same solvent ratio as initial solution and kept still for 4 h prior to DLS measurements; and another portion of solution was diluted to 0.25 mg g^{-1} copolymer concentration at predetermined DMF percentages for coordination mode studies by DLS.

Gel Permeation Chromatography (GPC) was performed on a PL-GPC120 setup being equipped with a column set consisting of two PL gel 5 μm MIXED-D columns (7.5 × 300 mm, effective molecular weight range of 0.2−400.0 kg mol^{-1}), using a DMF eluent that contained 0.01 mol L^{-1} LiBr at 80 °C at a flow rate of 1.0 mL min^{-1}. Narrowly distributed polystyrene standards in the molecular weight range of 0.5−7500.0 kg mol^{-1} (PSS, Mainz, Germany) were utilized for calibration.

Samples from polymerization were directly measured using diluted DMF solutions. For the coordination mode studies, the micelle-coordinated samples were prepared via evaporating the solvent from micellar solution, and the solids were dissolved in DMF under ultrasonication for 30 min and then filtered using 0.20 μm filters prior to GPC measurements.

Dynamic Light Scattering (DLS) Studies. Light scattering intensities and hydrodynamic diameters of solutions of copolymer micelles were measured on a BI-200SM Brookhaven instrument, equipped with a 100 mW adjustable solid-state laser emitting at 532 nm, a BI-200SM goniometer, and a BI-9000 digital correlator. The laser was adjusted to 43 mW, and a BI-TCD temperature controller was utilized to keep the solution precisely at 25 °C prior to measurements. Light scattering intensity at a fixed angle of 90° was recorded. The solutions were filtered using 0.20 μm filters prior to DLS measurements.

^{1}H NMR analyses were performed on a Bruker AV-400 NMR spectrometer. Samples were scanned for 32 times at 25 °C. All samples were fully dissolved or dispersed in deuterated solvents, e.g., D_2O, methanol-d_4, acetone-d_6, DMSO-d_6, or chloroform-*d*.

Transmission electron microscopy (TEM) was performed on a JEOL-1230 transmission electron microscope at an accelerating voltage of 100 kV. A droplet of solution was supported on a carbon-coated copper grid, dried in air at room temperature, and stained with 2% phosphotungstic acid solution.

Other Measurements. UV−vis spectra were recorded on a Perkin-Elmer lamda-25 UV−vis spectrometer at 25 °C. The visible light intensity was measured using a UV-A radiometer equipped with a 420 nm sensor. Solution pH was measured using a PHS-3C digital pH meter.

Results and Discussion

Inspired by the tunability of coordination mode in natural zinc proteins, this paper describes a new type of copolymer micelle, whose coordination mode may be finely tuned by the solution media. As illustrated in Figure 1, cobalt ions may coordinate with the functionalities of DBHHMA units in two different modes: one is the intrachain coordination mode, i.e., cobalt ions coordinate with the neighboring functionalities within a single PDBHHMA chain, in which the coordinated copolymer may be well dissolved in good solvent. Another is the interchain coordination mode, in which the PDBHHMA chains are cross-linked, and micelles are stabilized by this coordination

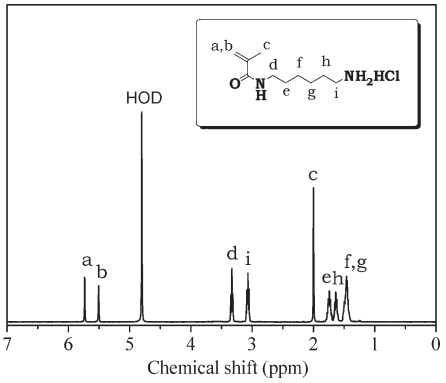

Figure 2. ^{1}H NMR spectrum of 6-aminohexylmethacrylamide hydrochloride (AHMA) monomer salt in D_2O.

cross-linking. Thus, the coordination mode selectivity facilitates to convert polymer micelles into noncrosslinking-coordinated state or stabilized state through coordination crosslinking. This leads to essentially different stability or permeability of polymer micelles in the nonselective good solvent.

Synthesis of PDBHHMA-*b*-PHEMA Copolymer. As shown in Scheme 1, the targeted PDBHHMA-*b*-PHEMA block copolymer was synthesized first via visible light activating RAFT polymerization of HEMA monomer at 25 °C, and then chain-extension RAFT polymerization of 6-aminohexyl methacrylamide hydrochloride (AHMA) monomer salt using the above-synthesized PHEMA as a macromolecular chain transfer agent (macro-CTA), under the same mild conditions. After chain-extension polymerization, the solution was directly reacted with 3,5-di-*tert*-butyl-2-hydroxybenzaldehyde to give PDBHHMA-*b*-PHEMA copolymer.

AHMA monomer was synthesized by the amidation of hexylenediamine monohydrochloride salt with methacryloyl chloride at −30 °C. As shown in Figure 2, the integral ratio of proton signals of I_a:I_b:I_d:I_i:I_c:I_e:I_h:I_{f+g} equals 1:1:2:2:3:2:2:4, within the analysis errors. This integral ratio is well comparable to the proton ratio of the targeted AHMA monomer salt. Moreover, except the signal of HOD, no signal of other impurities is detectable. This suggests the high purity of AHMA monomer.

PHEMA was synthesized via RAFT polymerization of HEMA monomer, using a CPFDB chain transfer agent and a TPO photoinitiator, at a feed molar ratio of $[HEMA]_0$:$[CPFDB]_0$:$[TPO]_0$ = 200:1:0.25 in 45 wt % DMF, under the visible light radiation at 25 °C. 52.5% HEMA monomer was polymerized in 3.5 h, according to ^{1}H NMR analysis.

As shown in the bottom spectrum of Figure 3a, no signal at δ = 5.5−6.5 ppm ($C\mathbf{H}_2$=CCH_3 of HEMA monomer) is detectable. This indicates that HEMA monomer was completely removed from this PHEMA sample. The integral ratio of proton signals of I_a:I_b:I_c:I_e:I_{d+h} = 1:2:2:2:3, which is comparable to the proton ratio of PHEMA. Except the signal of HOD, no signal of other impurities is detectable, indicating the high purity of this PHEMA sample. Moreover, as shown in the inset of Figure 3a, the signals at δ = 7.2−8.0 ppm ($FC_6\mathbf{H}_4CSS$ of CPFDB residues at PHEMA chain ends) are detectable. Thus, its degree of polymerization (DP) was assessed to be 120 according to eq 1:

$$\mathrm{DP} = \frac{I_b + I_c}{I_f + I_g} \quad (1)$$

As shown in Figure 3b, GPC trace of this PHEMA sample is quite narrow and symmetrical, suggesting the well-controlled

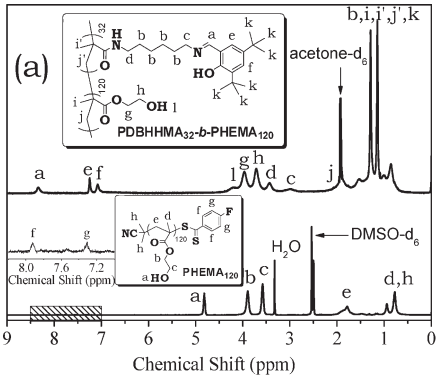

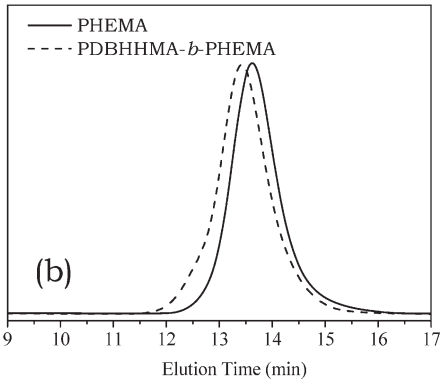

Figure 3. (a) ^{1}H NMR spectra and (b) GPC traces of poly(2-hydroxyethyl methacrylate) and its chain-extended poly[*N*-(6-(3,5-di-*tert*-butyl-2-hydroxybenzylideneamino)hexyl)methacrylamide]-*block*-poly(2-hydroxyethyl methacrylate) (PDBHHMA-*b*-PHEMA) copolymer.

behavior of this RAFT polymerization. Thus, it is a suitable macro-CTA for the chain extension RAFT polymerization of AHMA monomer salt.

To avoid the amonolysis of the chain-end dithioester CPFDB residues, the polymerization of AHMA monomer salt was performed in acidic water/DMF at solution pH 1.5−2.0, which was slightly lower than pK_a of 2.51 as assessed by titration analysis, at which the ammonium salt of AHMA starts to deionize. After this chain extension polymerization, 3,5-di-*tert*-butyl-2-hydroxybenzaldehyde was directly added in this solution. The pink solution changed to yellow upon adjusting to pH 10 at 25 °C. This mixture was stirred at 25 °C for 16 h to ensure the fulfillment of this reaction.

As shown in the upper spectrum of Figure 3a, the integral ratio of I_a:I_c is 1:2, suggesting the essentially complete reaction of primary amine functionalities of PAHMA blocks with 3,5-di-*tert*-butyl-2-hydroxybenzaldehyde. Except the signal of acetone-d_6 impurities, no signal of other impurities is detectable, indicating the high purity of this copolymer. Therefore, this copolymer was assessed to be $PDBHHMA_{32}$-*b*-$PHEMA_{120}$, according to eq 2:

$$\frac{I_{l+g+h+d}}{I_a} = \frac{5 \times 120 + 2\mathrm{DP}}{\mathrm{DP}} \quad (2)$$

where DP is the degree of polymerization of PDBHHMA blocks, I_a is the integral of proton signal at δ = 8.34 ppm (CH_2N=$C\mathbf{H}$ of PDBHHMA blocks), $I_{l+g+h+d}$ is the integral of proton signal at δ = 3.27−4.49 ppm ($C\mathbf{H}_2C\mathbf{H}_2O\mathbf{H}$ of PHEMA blocks and $CONHC\mathbf{H}_2$ of PDBHHMA blocks). 120 is the above-assessed degree of polymerization of PHEMA blocks. Moreover, GPC trace of $PDBHHMA_{32}$-*b*-$PHEMA_{120}$ copolymer is narrow and symmetrical (see Figure 3b), with a low M_w/M_n of 1.13.

Table 1. Dynamic Light Scattering Results of 1.0 mg g^{-1} PDBHHMA$_{32}$-*b*-PHEMA$_{120}$ Micellar Solutions in Mixed Solvents

solvent ratio	intensity (kcps)	D_h (nm)	polydispersity (μ_2/Γ^2)
W_{DMF}:$W_{methanol}$ = 10:90	23.7	27	0.035
W_{DMF}:$W_{methanol}$ = 5:95	33.9	24	0.092
W_{DMF}:W_{DCM} = 5:95	161	81	0.113

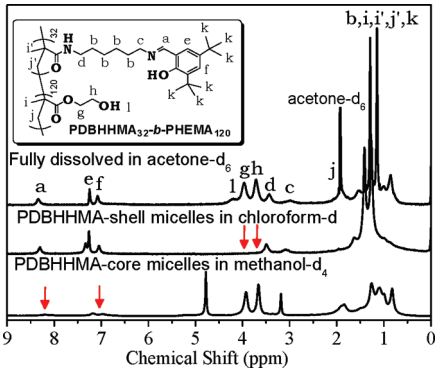

Figure 4. ^{1}H NMR spectra of PDBHHMA$_{32}$-*b*-PHEMA$_{120}$ copolymer separately (upper) in acetone-d_6, (middle) in chloroform-*d*, and (bottom) in methanol-d_4. Arrows indicate the attenuated signals.

Micellization of PDBHHMA$_{32}$-*b*-PHEMA$_{120}$ Copolymer. As shown in Table 1, in methanol solution at 5 wt % DMF, this block copolymer self-assembled into small micelles of hydrodynamic diameter D_h = 24 nm and low polydispersity μ_2/Γ^2 = 0.092; increasing DMF content to 10 wt % led to the swollen micelles with ca. 3 nm larger D_h and ca. 10 kcps lower intensity than the former. In contrast, in dichloromethame (DCM) solution at 5 wt % DMF, this copolymer self-assembled into larger inversed micelles of D_h = 81 nm and remarkably higher intensity of 161 kcps of solution.

As shown in Figure 4, as compared with ^{1}H NMR spectrum of fully dissolved copolymer in acetone-d_6 (nonselective solvent, upper spectrum), the proton signals of PHEMA blocks are fully detectable, but those of PDBHHMA blocks are attenuated in methanol-d_4 (selective solvent, bottom spectrum). This suggests the formation of PDBHHMA-core micelles in methanol. In contrast, the proton signals of PDBHHMA blocks are fully detectable but those of PHEMA blocks are attenuated in chloroform-*d* (selective solvent, middle spectrum). This suggests the formation of PDBHHMA-shell micelles in DCM.

Coordination of Cobalt Ions with PDBHHMA Blocks in Micellar Cores. It is well-known that the Co^{2+}−salen complexes rapidly oxidize to Co^{3+}−salen complexes on exposure in air.[60] Rossbach et al.[27] demonstrated that Co^{2+}−salen functionalities of block copolymers in micellar cores immediately converted to Co^{3+}−salen functionalities on exposure to air at room temperature. However, this oxidation leads to more ligand number but does not cleave the coordination bonds of Co−O or Co−N of salen functionalities. Thus, in the case of coordination of cobalt ions with the functionalities of PDBHHMA blocks, this oxidation does not change the inter- or intrachain coordination mode. Accordingly, the coordination experiments were carried out directly in air atmosphere.

As shown in Figure 5a, in methanol solution (5 wt % DMF), addition of cobalt acetate leads to the colorless solution gradually changes to brown. A typical coordination absorption at λ_{max} = 375 nm appears and gradually increases. As shown in the inset of Figure 5a, the absorption curve levels off in ca. 4800 s. This absorbance attributes to

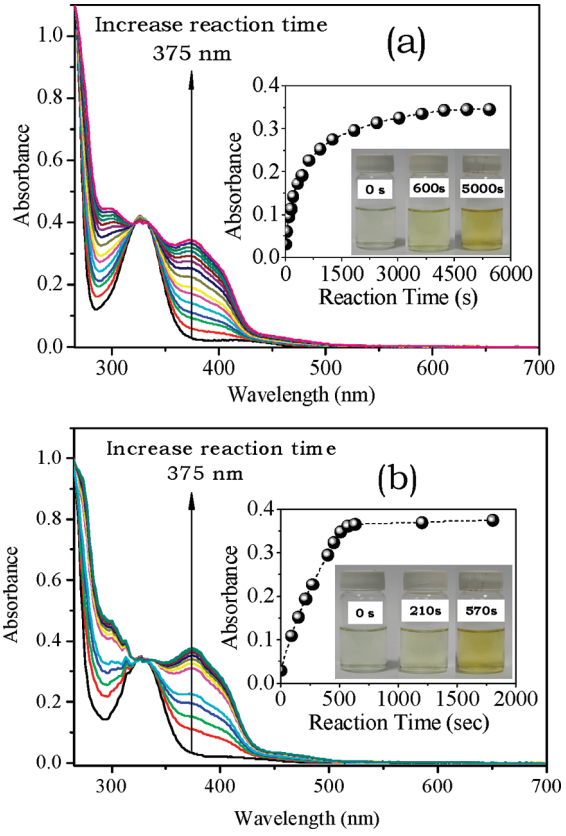

Figure 5. UV−vis spectroscopic evolution of a 0.125 mg g^{-1} PDBHHMA-core micellar solution of PDBHHMA$_{32}$-*b*-PHEMA$_{120}$ upon coordination with cobalt ions at a $[Co^{2+}]_0/[DBHHMA]_0$ = 0.60, (a) in methanol (5 wt % DMF) or (b) in methanol (10 wt % DMF). Inset: the absorbance at λ_{max} = 375 nm as a function of reaction time and solution photos at predetermined intervals.

Co^{2+}−DBHHMA$_2$ and Co^{3+}−DBHHMA$_2$ functionalities. Clearly, the coordination was controlled by the diffusion process of cobalt ions into hydrophobic micellar cores of PDBHHMA blocks. Considering the slower diffusion process and more rapid oxidation, the critical time of ca. 4800 s may be regarded as the time needed for fulfillment of coordination.

As shown in Figure 5b, coordination in methanol solution at 10 wt % DMF proceeds much more rapidly than at 5 wt % DMF; the solution changes to brown shortly in 570 s. As assessed from the inset of Figure 5b, this coordination carried out in ca. 490 s. Clearly, increasing DMF content inevitably leads to the swelling of PDBHHMA micellar cores. In addition, DMF may also well interact with cobalt ions, thus improves the compatibility of cobalt ions with hydrophobic PDBHHMA blocks. Both effects facilitate the diffusion of cobalt ions into hydrophobic micellar cores.

The coordination efficiency was further investigated by UV−vis spectroscopy. The coordinated solution was stirred in air at 20 °C for 12 h and kept still for 4 h to ensure complete oxidation. Thus, the absorbance at λ_{max} = 375 nm predominantly attributes to the absorption of Co^{3+}−DBHHMA$_2$ complexes. As shown in Figure 6, increasing the feed molar ratio of $[Co^{2+}]_0/[DBHHMA]_0$ leads to the linear increase of this absorbance at the low ratios and levels off at $[Co^{2+}]_0/[DBHMMA]_0$ of 0.37 in methanol solution at 5 wt % DMF or 0.40 in methanol solution at 10 wt % DMF. Because of the semistructural character of salen ligands[38] of PDBHHMA functionalities, one portion of cobalt ions most presumably coordinates with two portions of DBHHMA units. Thus,

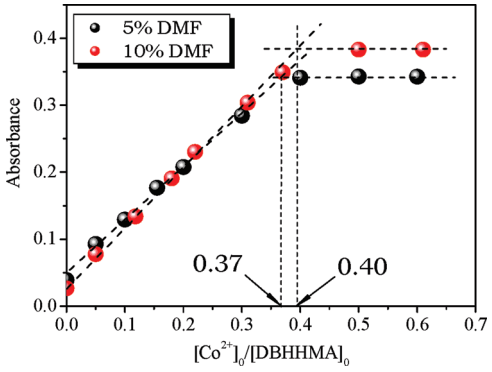

Figure 6. Evolution of absorbance at λ_{max} = 375 nm of a 0.125 mg g^{-1} of the coordinated PDBHHMA-core micellar solution of PDBHHMA$_{32}$-*b*-PHEMA$_{120}$ in methanol at 5 or 10 wt % DMF, upon increasing the feed molar ratio of $[Co^{2+}]_0/[DBHHMA]_0$.

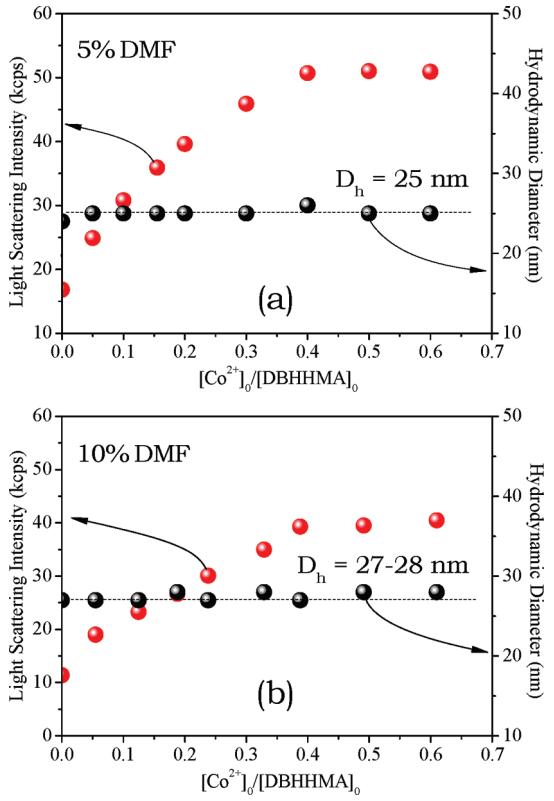

Figure 7. Dynamic light scattering results of 0.5 mg g^{-1} of the coordinated PDBHHMA-core micellar solution of PDBHHMA$_{32}$-*b*-PHEMA$_{120}$, (a) in methanol (5 wt % DMF) or (b) in methanol (10 wt % DMF), as a function of $[Co^{2+}]_0/[DBHHMA]_0$.

coordination efficiency of DBHHMA units is separately 74% at 5 wt % DMF or 80% at 10 wt % DMF. Considering the chain nature of PDBHHMA blocks, such high efficiency implies that this coordination occurs in the whole hydrophobic micellar cores rather than just at the core−shell interfaces.

As shown in Figure 7a, upon coordination in methanol solution at 5 wt % DMF, the size of micelles keeps essentially constant at D_h = 25 nm, but the light scattering intensity of solution increases from initially 16.8 kcps to 50 kcps at $[Co^{2+}]_0/[DBHHMA]_0$ = 0.4, at which ca. 80% DBHHMA units was coordinated, further increasing $[Co^{2+}]_0/[DBHHMA]_0$ does not lead to intensity increase. This suggests that this coordination was saturated at ca. 80% DBHHMA units coordinated. As shown in Figure 7b, upon coordination in methanol solution at 10 wt % DMF, D_h also keep constant at

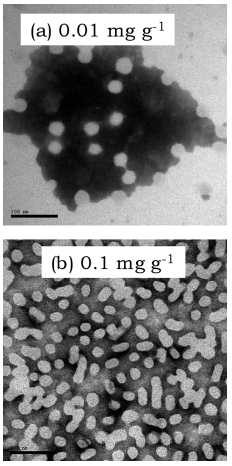

Figure 8. TEM images of the PDBHHMA-core micelles of PDBHHMA$_{32}$-*b*-PHEMA$_{120}$ copolymer coordinated at $[Co^{2+}]_0/[DBHHMA]_0$ = 0.60, from (a) 0.01 mg g^{-1} copolymer solution in methanol (0.01 wt % DMF) or (b) 0.1 mg g^{-1} copolymer solution in methanol (0.1 wt % DMF). Scale bar: 100 nm.

27−28 nm. The light scattering intensity increases from the initially 11.4 kcps to 40.5 kcps at $[Co^{2+}]_0/[DBHHMA]_0$ = 0.4. Clearly, this intensity increase is less pronounced than that at 5 wt % DMF. This indicates that the coordinated micelles are less compact at 10% DMF than at 5 wt % DMF.

As shown in Figure 8a, TEM image of negatively phosphotungstic acid-stained samples from 0.01 mg g^{-1} diluted methanol solution exhibits narrow-distributed spherical micelles with well-defined diameters of 24−26 nm. As shown in Figure 8b, increasing the copolymer concentration up to 0.1 mg g^{-1} tends to the fusion of micelles to nanorods with diameter the same as initial spherical micelles from dilute solution, no large spherical aggregate is detectable. This suggests the fusion of micellar shell domains; i.e., the coordination-crosslinked cores suppress the fusion of whole micelles in the precence of DMF solvent.

Studies on Coordination Modes in Micellar Cores. Because of same chemical environment and electron structural character of these coordinating sites, the spectroscopy or ^{1}H NMR cannot be utilized for the characterization of inter- or intrachain coordination mode. Fortunately, the inter- or intrachain coordination mode leads to different stability of micelles in nonselective good solvent. The intrachain-coordinated micelles may molecularly dissolve in good solvent, but interchain coordination leads to the coupling and crosslinking of polymer chains; such micelles cannot dissociate in good solvent or at least enlarge molecular weight of polymer. Thus, the stability of coordinated micelles in good solvent; e.g., DMF may well reflect the inter- or intrachain coordination mode.

As shown in Figure 9a, in the case of the initial methanol solution (5 wt % DMF) at low feed molar ratio of $[Co^{2+}]_0/[DBHHMA]_0$ = 0−0.05, increasing DMF content leads to the intensity decrease, which is close to that of the fully dissoved noncoordinated copolymer at 50 wt % DMF, suggesting the full dissolution of copolymer. This intensity decrease slows down upon increasing $[Co^{2+}]_0/[DBHHMA]_0$ to 0.155, at which the intensity is larger than 10 kcps even at 50 wt % DMF, suggesting the interchain coordination. As shown in Figure 9b, at $[Co^{2+}]_0/[DBHHMA]_0$ = 0−0.10, the micelles were dissociated at relatively high content of DMF. However, at $[Co^{2+}]_0/[DBHHMA]_0 \geq 0.155$, D_h of micelles kept essentially constant even at 50 wt % DMF. This confirms the formation of interchain coordination.

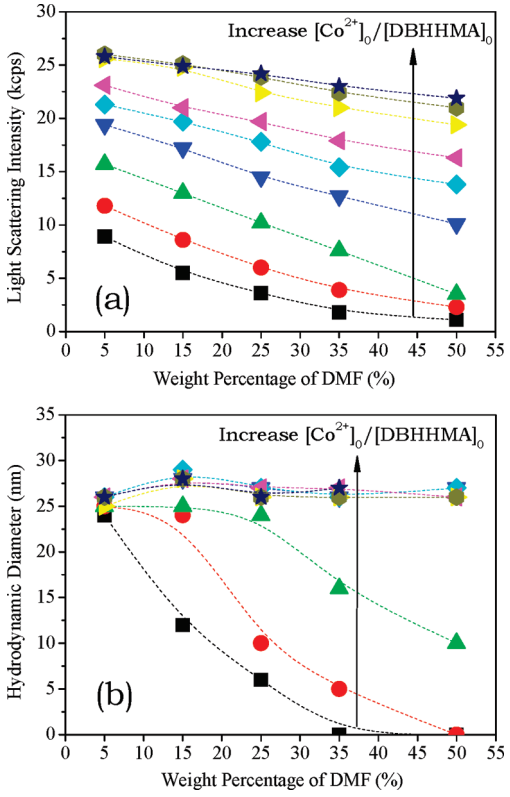

Figure 9. Dynamic light scattering results of the methanol solutions of PDBHHMA-core-coordinated copolymer micelles upon diluted by DMF. From bottom to up: at $[Co^{2+}]_0/[DBHHMA]_0$ = 0, 0.05, 0.10, 0.155, 0.20, 0.30, 0.40, 0.50, 0.60. Sample preparation: the initial 0.50 mg g^{-1} PDBHHMA-core-coordinated micellar solution (5 wt % DMF) was separately diluted to 0.25 mg g^{-1} at predetermined weight percentages of DMF.

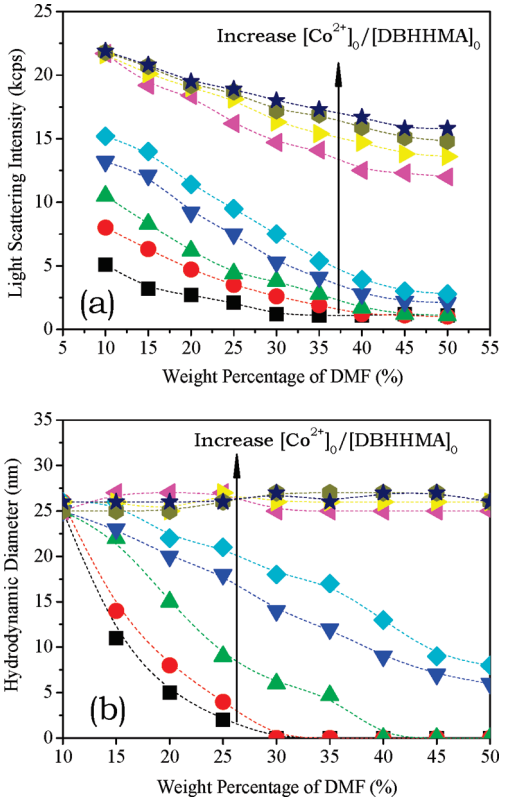

Figure 10. Dynamic light scattering results of the methanol solutions of PDBHHMA-core-coordinated copolymer micelles upon diluted by DMF. From bottom to up: at $[Co^{2+}]_0/[DBHHMA]_0$ = 0, 0.05, 0.118, 0.18, 0.22, 0.37, 0.50, 0.61, 0.72. Sample preparation: the initial 0.50 mg g^{-1} PDBHHMA-core-coordinated micellar solution (10 wt % DMF) was separately diluted to 0.25 mg g^{-1} at predetermined weight percentages of DMF.

As comparison, as shown in Figure 10, at $[Co^{2+}]_0/[DBHHMA]_0$ = 0−0.118, rapid decrease of intensity and D_h suggested that micelles were dissociated and copolymer was fully dissolved on increasing the fraction of DMF. At $[Co^{2+}]_0/[DBHHMA]_0$ = 0.18−0.22, micelles were dissociated to form irregular aggregates on addition of DMF. However, at $[Co^{2+}]_0/[DBHHMA]_0 \geq 0.37$, D_h of micelles kept essentially constant even at 50 wt % DMF. These critical ratios are much higher than those of coordinated micelles in methanol solution at 5 wt % DMF ($[Co^{2+}]_0/[DBHHMA]_0 \geq 0.155$), suggesting that the solvation effect of small amount of DMF leads to a tendency of intrachain coordination.

In summary, in methanol solution, the functionalities of hydrophobic PDBHHMA blocks in micellar cores tend to coordinate with cobalt ions in the interchain mode. A small amount of DMF remarkably accelerates this coordination but increases the tendency of intrachain coordination.

Coordination of Cobalt Ions in PDBHHMA-Shell Micelles. As shown in Figure 11, on the addition of cobalt ions in dichloromethane (DCM) solution of PDBHHMA-shell micelles, the colorless solution rapidly changes to brown. As shown in the inset of Figure 11, the coordination was fulfilled in ca. 50 s. This coordination proceeded remarkably more rapidly than in methanol solution at either 5 wt % DMF (ca. 4800 s) or 10 wt % DMF (ca. 490 s).

As shown in Figure 12, the absorbance at λ_{max} = 375 nm linearly increases with the feed molar ratio of $[Co^{2+}]_0/[DBHHMA]_0$. This coordination reaches a saturated point at $[Co^{2+}]_0/[DBHHMA]_0$ = 0.41, at which ca. 82% DBHHMA units were coordinated. This efficiency is in good agreement with the theoretical value of 81.45%, as assessed by the

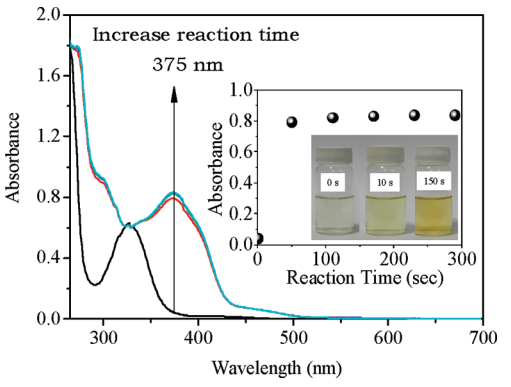

Figure 11. UV−vis spectroscopic evolution of a 0.125 mg g^{-1} PDBHHMA-shell micellar solution of $PDBHHMA_{32}$-*b*-$PHEMA_{120}$ in DCM (5 wt % DMF) upon the coordination with cobalt ions at a $[Co^{2+}]_0/[DBHHMA]_0$ = 0.60. Inset: absorbance at λ_{max} = 375 nm as a function of reaction time and solution photos at predetermined intervals.

computer simulation based on enumeration method assuming that all coordinations proceed in the intrachain mode (see Supporting Information).

As shown in Figure 13a, in DCM solution, upon coordination over a wide range of $[Co^{2+}]_0/[DBHHMA]_0$ = 0−0.70, both the size of micelles and light scattering intensity of solution are essentially constant. This indicates that the coordination does not affect the aggregation behavior; i.e., no or negligible interchain coordination occurs. This is totally contrary to the coordination of PDBHHMA blocks

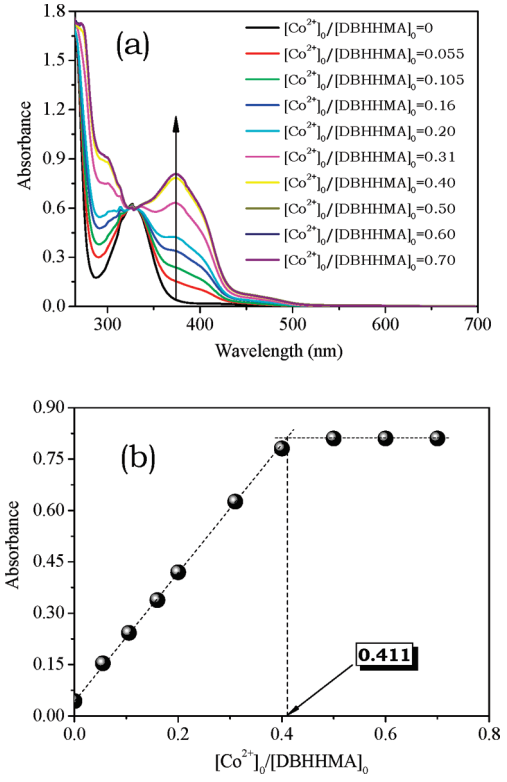

Figure 12. (a) UV−vis spectra of a 0.125 mg g^{-1} PDBHHMA-shell micellar solution of $PDBHHMA_{32}$-*b*-$PHEMA_{120}$ in DCM (5 wt % DMF) as a function of $[Co^{2+}]_0/[DBHHMA]_0$. (b) Evolution of absorbance at λ_{max} = 375 nm upon increasing the feed molar ratio of $[Co^{2+}]_0/[DBHHMA]_0$.

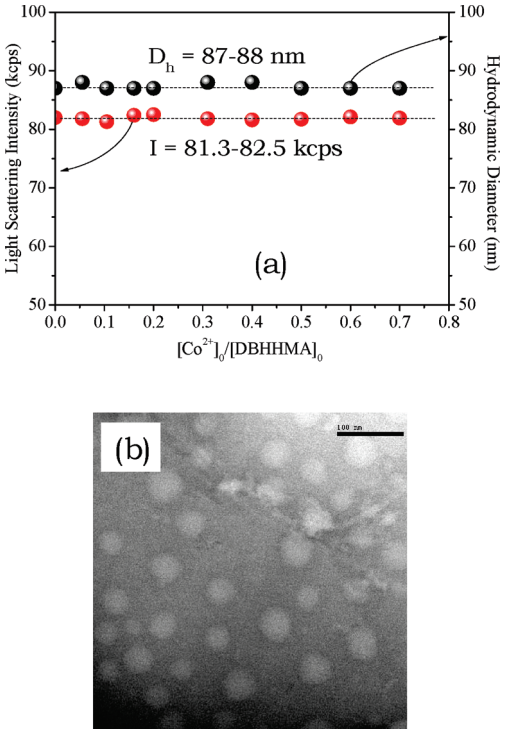

Figure 13. (a) Dynamic light scattering results of a 0.5 mg g^{-1} of the coordinated micellar solution of $PDBHHMA_{32}$-*b*-$PHEMA_{120}$ in DCM (5 wt % DMF) as a function of $[Co^{2+}]_0/[DBHHMA]_0$. (b) TEM image of the coordinated micelles from 0.1 mg g^{-1} copolymer solution in DCM (1 wt % DMF). Scale bar: 100 nm.

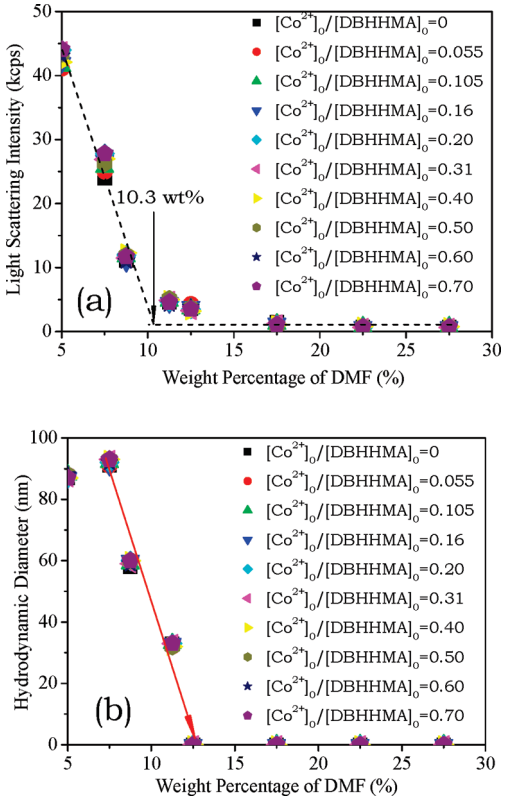

Figure 14. Dynamic light scattering results of the DCM solutions of PDBHHMA-shell-coordinated copolymer micelles upon diluted by DMF. Sample preparation: the initial DCM solution of 0.50 mg g^{-1} PDBHHMA-shell-coordinated micelles (5 wt % DMF) was separately diluted to 0.25 mg g^{-1} at predetermined weight percentages of DMF.

in micellar cores where more compact micelles formed as indicated by the intensity increase (see Figure 7). As shown in Figure 13b, these aggregates are large spherical micelles, rather than vesicles or other types of aggregates.

As shown in Figure 14a, adding DMF may lead to a sharp decrease of both light scattering intensity and D_h. No aggregate is detectable at 10.3 wt % DMF, even large excess of cobalt ions added, e.g., $[Co^{2+}]_0/[DBHHMA]_0 = 0.70$. This confirms the intrachain coordination. This phenomenon is totally different from what observed in the covalently shell-crosslinked polymer micelles,[61−64] in which large excess of cross-linkers inevitably leads to the shell-crosslinking due to the highly concentrated polymer chains in micellar shells.

GPC Evidence for Coordination Modes in PDBHHMA-*b*-PHEMA Micelles. Prior to GPC measurements, the solvent of micellar solutions were first evaporated, the solids were redissolved in DMF, and large aggregates were removed by filtration using 0.20 μm filters. For the samples from PDBHHMA-shell-coordinated micelles, the light scattering intensities of solution before and after filtration are essentially the same as 0.7−0.9 kcps. Moreover, GPC pump keeps normal pressure the same as initially 10.7 MPa on measurements. This suggests that the coordinated micelles were molecularly dissolved in DMF.

In contrast, for the samples from PDBHHMA-core-coordinated micelles, particularly those at $[Co^{2+}]_0/[DBHHMA]_0 \geq 0.15$, the filtration process leads to a dramatical decrease of light scattering intensity, e.g., from initially 19 kcps down to 3.2 kcps. Moreover, the pressure of GPC pump increases from initially 10.7 MPa up to strikingly 13.8 MPa on measurement. This suggests the formation of insoluble large aggregates.

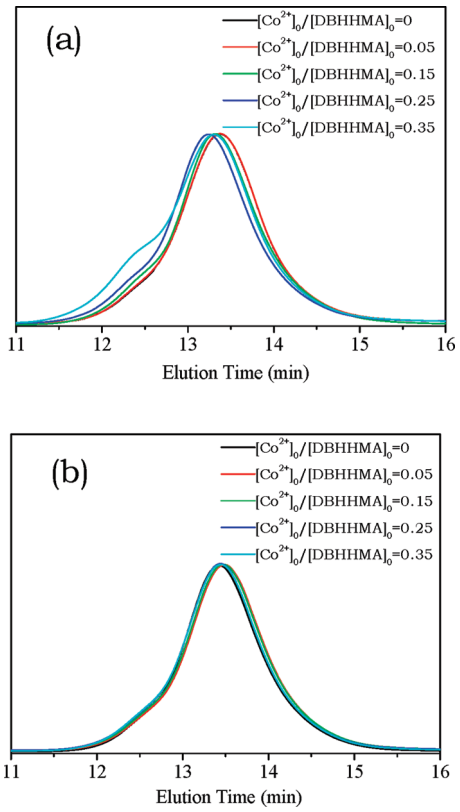

Figure 15. GPC traces of the coordinated $PDBHHMA_{24}$-*b*-$PHEMA_{120}$ copolymer samples: (a) from methanol solutions (5 wt % DMF) of PDBHHMA-core-coordinated micelles; (b) from DCM solutions (5 wt % DMF) of PDBHHMA-shell-coordinated micelles. The samples were prepared via separately evaporating solvents from micellar solutions, dissolving the solids in DMF, and filtering by 0.20 μm filters prior to measurements.

As shown in Figure 15a, GPC trace of the samples from PDBHHMA-core-coordinated micelles at $[Co^{2+}]_0/[DBHHMA]_0 = 0.05$ is essentially the same as that of noncoordinated copolymer. This indicates the intrachain coordination. However, at $[Co^{2+}]_0/[DBHHMA]_0 \geq 0.15$, new shoulders at high molecular weight side of their GPC traces are detectable, despite large aggregates were removed prior to mesurements. This demonstrates significant amount of interchain coordination. On the contrary, for the samples from PDBHHMA-shell-coordinated micelles, all GPC traces are essentially the same as noncoordinated copolymer (Figure 15b), even at large excess of cobalt ions, e.g. $[Co^{2+}]_0/[DBHHMA]_0 = 0.70$. This confirms the predominant intrachain coordination.

Conclusions

This paper describes a new type of polymer micelle, whose coordination mode may be well tuned simply via adjusting the solution media. To this end, a well-defined PDBHHMA-*b*-PHEMA copolymer was synthesized via visible light activating RAFT polymerization of HEMA monomer at 25 °C, and chain-extension RAFT polymerization of AHMA monomer salt, and finally reacted directly with 3,5-di-*tert*-butyl-2-hydroxybenzaldehyde. ^{1}H NMR and GPC analyses confirmed the intact structure, well-defined molecular weight, and narrow molecular weight distribution of this block copolymer.

$PDBHHMA_{32}$-*b*-$PHEMA_{120}$ copolymer could self-assemble into small PDBHHMA-core micelles in methanol or large inversed PDBHHMA-shell micells in DCM. Both types of micelles could well coordinate with cobalt ions in the whole PDBHHMA micellar shells or cores. The coordination of PDBHHMA blocks in micellar shells proceeded much more rapidly than that in micellar cores. The addition of small amount of DMF significantly accelerated the coordination process in micellar cores. Upon coordination, the size of micelles kept essentially constant, but the light scattering intensity of methanol solution of PDBHHMA-core micelles linearly increased up to a critical ratio of $[Co^{2+}]_0/[DBHHMA]_0 = 0.4$; a small amount of DMF brought down this intensity increase. However, this coordination did not change the light scattering intensity of DCM solution of PDBHHMA-shell micelles, even at $[Co^{2+}]_0/[DBHHMA]_0 = 0.7$.

Both DLS and GPC results evidenced that cobalt ions tended to coordinate with the functionalities of PDBHHMA blocks in micellar cores in the interchain mode; the addition of a small amount of DMF led to the tendency of intrachain coordination. In contrast, cobalt ions predominantly coordinated with the functionalities of PDBHHMA blocks in micellar shells in the intrachain mode. This media-modulated selectivity of coordination modes may not only well adjust the stability of micelles but also finely tune the permeability of these polymer micelles. These properties are going to be reported in a follow-up paper but are beyond the scope of this paper.

Acknowledgment. We thank National Natural Science Foundation of China (20874081, 20674064), Research Fund for Doctoral Program of Higher Education of China (200805300004), and Scientific Research Fund of Hunan Provincial Education Department for financial support of this research. We thank Prof. Lifeng Tan for the helpful discussion on coordination studies.

Supporting Information Available: Computer simulation of coordination in the intrachain mode on the basis of the enumeration method. This material is available free of charge via the Internet at http://pubs.acs.org.

References and Notes

(1) Chen, D.; Jiang, M. *Acc. Chem. Res.* **2005**, *38*, 494–502.
(2) Hofmeier, H.; Schubert, U. S. *Chem. Commun.* **2005**, 2423–2432.
(3) Cho, J.; Hong, J.; Char, K.; Caruso, F. *J. Am. Chem. Soc.* **2006**, *128*, 9935–9942.
(4) Weaver, J. V. M.; Tang, Y.; Liu, S.; Iddon, P. D.; Grigg, R.; Billingham, N. C.; Armes, S. P.; Hunter, R.; Rannard, S. P. *Angew. Chem., Int. Ed.* **2004**, *43*, 1389–1392.
(5) Bronich, T. K.; Keifer, P. A.; Shlyakhtenko, L. S.; Kabanov, A. V. *J. Am. Chem. Soc.* **2005**, *127*, 8236–8237.
(6) Chen, B.; Sleiman, H. F. *Macromolecules* **2004**, *37*, 5866–5872.
(7) Pan, D.; Caruthers, S. D.; Hu, G.; Senpan, A.; Scott, M. J.; Gaffney, P. J.; Wickline, S. A.; Lanza, G. M. *J. Am. Chem. Soc.* **2008**, *130*, 9186–9187.
(8) Cai, Y.; Armes, S. P. *Macromolecules* **2004**, *37*, 7116–7122.
(9) Pollino, J. M.; Weck, M. *Chem. Soc. Rev.* **2005**, *34*, 193–207.
(10) South, C. R.; Burd, C.; Weck, M. *Acc. Chem. Res.* **2007**, *40*, 63–74.
(11) Loginova, T. P.; Kabachii, Y. A.; Sidorov, S. N.; Zhirov, D. N.; Valetsky, P. M.; Ezernitskaya, M. G.; Dybrovina, L. V.; Bragina, T. P.; Lependina, O. L.; Stein, B.; Bronstein, L. M. *Chem. Mater.* **2004**, *16*, 2369–2378.
(12) Wang, H.; Patil, A. J.; Liu, K.; Petrov, S.; Mann, S.; Winnik, M. A.; Manners, I. *Adv. Mater.* **2009**, *21*, 1805–1808.
(13) Schubert, U. S.; Eschbaumer, C. *Macromol. Symp.* **2001**, *163*, 177–187.
(14) Gohy, J.-F.; Lohmeijer, B. G. G.; Schubert, U. S. *Macromol. Rapid Commun.* **2002**, *23*, 555–560.
(15) Gohy, J.-F.; Lohmeijer, B. G. G.; Schubert, U. S. *Macromolecules* **2002**, *35*, 4560–4563.
(16) Gohy, J.-F.; Lohmeijer, B. G. G.; Varshney, S. K.; Schubert, U. S. *Macromolecules* **2002**, *35*, 7427–7435.
(17) Gohy, J.-F.; Lohmeijer, B. G. G.; Varshney, S. K.; Décamps, B.; Leroy, E.; Boileau., S.; Schubert, U. S. *Macromolecules* **2002**, *35*, 9748–9755.
(18) Gohy, J.-F.; Lohmeijer, B. G. G.; Schubert, U. S. *Chem.—Eur. J.* **2003**, *9*, 3472–3479.

(19) Guillet, P.; Fustin, C.-A.; Lohmeijer, B. G. G.; Schubert, U. S.; Gohy, J.-F. *Macromolecules* **2006**, *39*, 5484–5488.
(20) Guillet, P.; Fustin, C.-A.; Mugemana, C.; Ott, C.; Schubert, U. S.; Gohy, J.-F. *Soft Matter* **2008**, *4*, 2278–2282.
(21) Ott, C.; Hoogenboom, R.; Hoeppener, S.; Wouters, D.; Gohy, J.-F.; Schubert, U. S. *Soft Matter* **2009**, *5*, 84–91.
(22) Guillet, P.; Fustin, C.-A.; Wouters, D.; Hoeppener, S.; Schubert, U. S.; Gohy, J.-F. *Soft Matter* **2009**, *5*, 1460–1465.
(23) Gohy, J.-F.; Ott, C.; Hoeppenerb, S.; Schubert, U. S. *Chem. Commun*. **2009**, 6038–6040.
(24) Guillet, P.; Mugemana, C.; Stadler, F. J.; Schubert, U. S.; Fustin, C.-A.; Bailly, C.; Gohy, J.-F. *Soft Matter* **2009**, *5*, 3409–3411.
(25) Zarka, M. T.; Bortenschlager, M.; Wurst, K.; Nuyken, O.; Weberskirch, R. *Organometallics* **2004**, *23*, 4817–4820.
(26) Schönfelder, D.; Fischer, K.; Schmidt, M.; Nuyken, O.; Weberskirch, R. *Macromolecules* **2005**, *38*, 254–262.
(27) Rossbach, B. M.; Leopold, K.; Weberskirch, R. *Angew. Chem., Int. Ed*. **2006**, *45*, 1309–1312.
(28) Pressly, E. D.; Rossin, R.; Hagooly, A.; Fukukawa, K.-i.; Messmore, B. W.; Welch, M. J.; Wooley, K. L.; Lamm, M. S.; Hule, R. A.; Pochan, D. J.; Hawker, C. J. *Biomacromolecules* **2007**, *8*, 3126–3134.
(29) Sun, G.; Hagooly, A.; Xu, J.; Nyström, A. M.; Li, Z.; Rossin, R.; Moore, D. A.; Wooley, K. L.; Welch, M. J. *Biomacromolecules* **2008**, *9*, 1997–2006.
(30) Noonan, K. J. T.; Gillon, B. H.; Cappello, V.; Gates, D. P. *J. Am. Chem. Soc*. **2008**, *130*, 12876–12877.
(31) Yan, Y.; Besseling, N. A. M.; de Keizer, A.; Marcelis, A. T. M.; Drechsler, M.; Stuart, M. A. C. *Angew. Chem., Int. Ed*. **2007**, *46*, 1807–1809.
(32) Ievins, A. D.; Moughton, A. O.; O'Reilly, R. K. *Macromolecules* **2008**, *41*, 3571–3578.
(33) Moughton, A. O.; O'Reilly, R. K. *J. Am. Chem. Soc*. **2008**, *130*, 8714–8725.
(34) Zhou, G.; He, J.; Harruna, I. I. *J. Polym. Sci., Polym. Chem*. **2007**, *45*, 4204–4210.
(35) Li, S.; Lin, M.; Lu, J.; Liang, H. *Macromolecules* **2009**, *42*, 1258–1263.
(36) Zhang, Y.; Gladyshev, V. N. *Chem. Rev*. **2009**, *109*, 4828–4861.
(37) Maret, W.; Li, Y. *Chem. Rev*. **2009**, *109*, 4682–4707.
(38) Madhavan, N.; Jones, C. W.; Weck, M. *Acc. Chem. Res*. **2008**, *41*, 1153–1165.
(39) Chiefari, J.; Chong, Y. K. B.; Ercole, F.; Krstina, J.; Jeffery, J.; Le, T. P. T.; Mayadunne, R. T. A.; Meijs, G. F.; Moad, C. L.; Moad, G.; Rizzardo, E.; Thang, S. H. *Macromolecules* **1998**, *31*, 5559–5562.
(40) Lokitz, B. S.; York, A. W.; Stempka, J. E.; Treat, N. D.; Li, Y.; Jarrett, W. L.; McCormick, C. L. *Macromolecules* **2007**, *40*, 6473–6480.
(41) McCormick, C. L.; Lowe, A. B. *Acc. Chem. Res*. **2004**, *37*, 312–325.
(42) Li, Y.; Smith, A. E.; Lokitz, B. S.; McCormick, C. L. *Macromolecules* **2007**, *40*, 8524–8526.
(43) Mertoglu, M.; Laschewsky, A.; Skrabania, K.; Wieland, C. *Macromolecules* **2005**, *38*, 3601–3614.
(44) Laschewsky, A.; Mertoglu, M.; Kubowicz, S.; Thünemann, A. F. *Macromolecules* **2006**, *39*, 9337–9345.
(45) McCullough, L. A.; Dufour, B.; Tang, C.; Zhang, R.; Kowalewski, T.; Matyjaszewski, K. *Macromolecules* **2007**, *40*, 7745–7747.
(46) Schilli, C. M.; Zhang, M.; Rizzardo, E.; Thang, S. H.; Chong, Y. K.; Edwards, K.; Karlsson, G.; Müller, A. H. E. *Macromolecules* **2004**, *37*, 7861–7866.
(47) Li, Y.; Lokitz, B. S.; Armes, S. P.; McCormick, C. L. *Macromolecules* **2006**, *39*, 2726–2728.
(48) Zhang, J.; Jiang, X.; Zhang, Y.; Li, Y.; Liu, S. *Macromolecules* **2007**, *40*, 9125–9132.
(49) Walther, A.; Millard, P.; Goldmann, A.; Lovestead, T.; Schacher, F.; Barner-Kowollik, C.; Müller, A. H. E. *Macromolecules* **2008**, *41*, 8608–8619.
(50) Smith, A. E.; Xu, X.; McCormick, C. L. *Prog. Polym. Sci*. **2010**, *35*, 45–93.
(51) Lu, L.; Yang, N.; Cai, Y. *Chem. Commun*. **2005**, 5287–5288.
(52) Lu, L.; Zhang, H.; Yang, N.; Cai, Y. *Macromolecules* **2006**, *39*, 3770–3776.
(53) Jiang, W.; Lu, L.; Cai, Y. *Macromol. Rapid Commun*. **2007**, *28*, 725–728.
(54) Li, Y.; Tang, Y.; Yang, K.; Chen, X.; Lu, L.; Cai, Y. *Macromolecules* **2008**, *41*, 4597–4606.
(55) Deng, J.; Shi, Y.; Jiang, W.; Peng, Y.; Lu, L.; Cai, Y. *Macromolecules* **2008**, *41*, 3007–3014.
(56) Sun, J.; Peng, Y.; Chen, Y.; Liu, Y.; Deng, J.; Lu, L.; Cai, Y. *Macromolecules* **2010**, *43*, 4041−4049.
(57) Shi, Y.; Gao, H.; Lu, L.; Cai, Y. *Chem. Commun*. **2009**, 1368–1370.
(58) Shi, Y.; Liu, G.; Gao, H.; Lu, L.; Cai, Y. *Macromolecules* **2009**, *42*, 3917–3926.
(59) Benaglia, M.; Rizzardo, E.; Alberti, A.; Guerra, M. *Macromolecules* **2005**, *38*, 3129–3140.
(60) Nishinaga, A.; Kondo, T.; Matsuura, T. *Chem. Lett*. **1985**, *14*, 905–908.
(61) Thurmond, K. B.; Kowalewski, T.; Wooley, K. L. *J. Am. Chem. Soc*. **1996**, *118*, 7239–7240.
(62) Liu, S.; Weaver, J. V. M.; Tang, Y.; Billingham, N. C.; Armes, S. P.; Tribe, K. *Macromolecules* **2002**, *35*, 6121–6131.
(63) Joralemon, M. J.; O'Reilly, R. K.; Hawker, C. J.; Wooley, K. L. *J. Am. Chem. Soc*. **2005**, *127*, 16892–16899.
(64) Liu, H.; Jiang, X.; Fan, J.; Wang, G.; Liu, S. *Macromolecules* **2007**, *40*, 9074–9083.